Food Chemistry: X 16 (2022) 100490

Contents lists available at ScienceDirect

Food Chemistry: X

journal homepage: www.sciencedirect.com/journal/food-chemistry-x

Preparation of bio-based modified starch film and analysis of preservation mechanism for sweet cherry

Jie Zhang [a,c,1], Lin Zhu [b,1], Kai-mian Li [c], Jianqiu Ye [c], Xinhui Xiao [c], Maofu Xue [c], Ming Wang [c], Yin-hua Chen [a,*]

[a] College of Tropical Crops, Hainan University, Haikou 570228, China
[b] College of Food Science and Technology, Hainan University, Haikou 570228, China
[c] Institute of Tropical Crop Genetic Resources, Chinese Academy of Tropical Agriculture Sciences, Haikou 571101, China

ARTICLE INFO

Keywords:
Octenyl succinate cassava starch ester
ε-Polylysine
Bio-based modified starch film
Characterization
Preservation

ABSTRACT

This study aimed to synthesize packaging films using bioactive ingredients. The composite film was prepared by blending octenyl succinate cassava starch ester (OSCS) with chitosan (CS) nano-ZnO and then adding ε-polylysine (ε-PL). The study also explored the effect of different concentrations of ε-PL on OSCS/CS/ZnO films. Fourier infrared spectroscopyand fluorescence microscopy revealed that the composite film was formed by both hydrogen bonding and a Schiff base reaction. The diffraction peaks of the original materials in X-ray diffraction disappeared after film formation, indicating good miscibility between the materials. Scanning electron microscope showed that the density of its structure increased with increasing the ε-PL content. The thermogravimetric analysis showed that the addition of ε-PL improved the thermal stability of the composite film to some extent. When used in cherry preservation, the bio-based modified starch film effectively reduced cherry decay, stem dryness, and weight loss, maintained surface color, and increased the soluble solid content.

Introduction

Sweet cherry (*Prunus avium L.*), native to western Asia and southeastern Europe (Giménez et al., 2016), is a fruit tree in the family Rosaceae, with small but colorful and nutritious fruits that are rich in carbohydrates and bioactive substances. Its pomace contains many active substances, mainly polyphenols, (Domínguez-Rodríguez, Marina, & Plaza, 2022) anthocyanins, and flavonoids. With excellent antioxidant properties (Blando & Oomah, 2019), it is one of the most popular temperate fruits. However, in the postharvest storage process, due to its thin skin and juiciness, it is susceptible to water loss, softening, browning, and pathogenic fungal erosion and decay (Pan et al., 2022). Therefore, it is important to find safe and effective packaging films for freshness preservation.

Today, cling films made from petroleum-based compounds still dominate the market but are problematic for many reasons. These plastic cling films are a major contributor to marine pollution, a problem that is worsening rapidly, with approximately 10–20 tons of plastic accumulating in the oceans globally each year (Sharma et al., 2022). Plastic films are also extremely difficult to degrade, and they release toxic gases such as dioxins, furans, mercury, and polychlorinated biphenyls, polluting the environment and causing aerosol poisoning (D. Wu et al., 2021). Plastic films are also highly susceptible to microbial contamination. Finally, they are non-renewable and generally not recyclable. For these reasons, the search for safe, degradable, and renewable cling films is imperative.

Polysaccharides can be used as environmentally friendly packaging materials (Ahmed M. Youssef & El-Sayed, 2018), octenyl succinate amylose was obtained by modifying natural starch (Cheng, Ai, & Ghosh, 2021) to give it several advantages over natural starch, such as improved amphiphilic properties and lower permeability to moisture, with the goal of improving its performance as a food packaging material. Chitosan is a natural polysaccharide obtained by deacetylation of chitin, which itself has good film-forming properties, biocompatibility, and degradability. Food grade chitosan is widely used in biopharmaceutical and health care and can be used to make hybrid films, such as (Wang, Huang et al., 2022) chitosan/zea alcohol soluble protein/tea polyphenol composite films have been applied to mushroom preservation (Q. Liu

* Corresponding author.
E-mail address: yhchen@hainanu.edu.cn (Y.-h. Chen).
[1] Jie Zhang and Lin Zhu has contributed to this manuscript.

https://doi.org/10.1016/j.fochx.2022.100490
Received 8 August 2022; Received in revised form 23 September 2022; Accepted 21 October 2022
Available online 25 October 2022

et al., 2022). Kynnipin cross-linked amphiphilic chitosan film has good UV resistance and compact structure, and it prolonged the shelf life of strawberries. (You et al., 2022) 1-methylcyclopropene composite chitosan overlay film was used to preserve passion fruit. The chitosan, antibacterial microcrystalline cellulose, and probiotic cultures formed a film that was used for cheese storage. After 45 days, the abundance of *Lactobacillus* in the coated cheese exceeded 8.00 log CFU/g compared with 6.35 log CFU/g in the pure control, which was advantageous for improving the cheese quality (El-Sayed, El-Sayed, Mabrouk, Nawwar, & Youssef, 2021). Nano-ZnO is a photocatalytic inorganic metal ion that inhibits microbial growth by combining with OH– to form a hydroxyl group with strong oxidative properties through photocatalysis. It has high heat resistance and low toxicity, and it can be used against a broad spectrum of microbes. It has a long inhibition cycle and no microbes have developed resistance to it. (Xie, Pan, & Cai, 2022) prepared antimicrobial cellulose-based films custom-built with ZnO nanopillars on the surface, and the films showed promise for use in food packaging. The films formed by adding Ag-NPs and Au-NPs to the chitosan solution had an excellent antibacterial effect and non-toxic properties (Ahmed M. Youssef, Abdel-Aziz, & El-Sayed, 2014). ZnO and SiO_2 formed composites, which were added to the films and improved Young's modulus of the films. Also, 5 wt% ZnO–SiO_2–NPs had the best tensile strength. It could form hydrophobic composites, inhibit flammability behavior, and improve antibacterial properties (Moustafa, Darwish, & Youssef, 2022). (El-Sayed, El-Sayed, & Youssef, 2021) *Lactobacillus* strains combined with zinc oxide to form nanoparticles had good antibacterial activity and positively affected the shelf life of yogurt. (Youssef, El-Sayed, El-Nagar, & El-Sayed, 2021) a film was prepared using carboxymethyl cellulose, gum arabic, and gelatin. The film contained garlic extract and titanium dioxide nanoparticles. TiO_2-NPs added to the film improved the film water vapor transmission rate, oxygen transmission rate, mechanical properties, and antimicrobial properties. The basic and antimicrobial properties were also improved, maintaining the quality of tilapia. The incorporation of silver@titanium oxide nanoparticles in cryogel formation enhanced the antimicrobial efficiency (El-Naggar et al., 2020). The incorporation of various nano ions improved the antimicrobial and mechanical properties of the films. ε-PL was added to the films to enhance their antimicrobial ability(Rahman, Konwar, Majumdar, & Chowdhury, 2021). ε-PL can be fermented by microbes to make a product with spectroscopic inhibitory activity against gram-negative bacteria, gram-positive bacteria, yeasts, and molds (Chang, Lu, Park, & Kang, 2010; Jiao et al., 2020). The addition of antimicrobial agents can achieve the goals of destroying spoilage and pathogenic bacteria (Jayakumar et al., 2022) that contaminate food, extending the shelf life, and ensuring food safety, all while meeting consumer requirements for nutrition, freshness, and taste. ε-PL has been used successfully as a food preservative in previous studies. (Alirezalu, Movlan, Yaghoubi, Pateiro, & Lorenzo, 2021) used ε-PL as a coating and added SNE (stinging nettle extract) to preserve fresh beef. (Wang, Sun et al., 2022) prepared ε-PL/gelatin/zeaxolysin nanofiber films to improve shelf life of frozen chicken breasts.

In this paper, octenyl succinate cassava starch ester (OSCS) was blended with chitosan (CS), nano-ZnO, and different concentrations of ε-PL to prepare modified starch films. The modified starch films were then subjected to structural analysis by scanning electron microscopy, Fourier infrared spectroscopy, full inverted fluorescence microscopy, thermogravimetric analysis and X-ray diffraction. The films were also applied to cherries to explore the potential applications of modified starch films in fruit and vegetable preservation for food packaging.

Materials and methods

Materials

Cassava starch and octenyl succinate cassava starch ester are self-made in the laboratory; Chitosan (degree of deacetylation ≥90 %) was purchased from Hefei Bomei Biotechnology Co., ltd; Octenylsuccinic anhydride comes from Guangzhou Guangjia Chemical Co., ltd; Zinc oxide (particle size 30 nm) comes from cool chemistry; Sodium hydroxide, glycerin, petroleum ether and absolute ethanol are all purchased from Xilong science; ε- Polylysine and hydrochloric acid came from Sinopharm Chemical Reagent Co., ltd. and PBS buffer was purchased from Lvyuan Biotechnology Co., ltd. All reagents are analytically pure. Sweet cherries were purchased from the orchard of Hainan University; The manufacturer of PE fresh-keeping film is yueshitang.

Preparation of modified starch film

We prepared five different solutions with different compositions: CS, OSCS, OSCS/CS, OSCS/CS/ZnO, and OSCS/CS/ZnO with different concentrations of ε-PL. A 2 % concentration CS solution was first prepared by dissolving chitosan (CS) in 1 % (m/V) acetic acid solution using a magnetic stirrer at 50 °C with constant stirring for 2 h. A 2 % concentration OSCS solution was prepared by gelatinizing octenyl succinate cassava starch ester (OSCS) at 80 °C for 15 min with constant stirring. To make the OSCS/CS solution, the prepared CS and OSCS solutions were each mixed with 0.98 % glycerol (m/V, where V is the volume of total film solution) and then were combined with a mass ratio of 1:1 (m/m) between the OSCS solution and the CS solution.

To make the OSCS/CS/ZnO solution, 1.9 % (m/M, where M is the mass dry weight of starch and chitosan) nano-ZnO was added to the OSCS/CS solution. To make the OSCS/CS/ZnO/ε-PL solutions, 0 %, 2 %, 4 %, 6 %, or 8 % ε-PL (m/M, M mass dry weight of starch and chitosan) was added to the OSCS/CS/ZnO solution.

The above solutions were physically co-mixed for 2 h until the solutions were completely uniform and then degassed by sonication in an ultrasonic cleaner for 40 min. Finally, to make the films, the degassed solutions were cast in a mold and dried at 50 °C for 24 h.

FT-IR spectral analysis of modified starch film

Changes in the chemical structure of the modified starch films were analyzed using an infrared spectrometer (BRUKER, Germany) in ATR mode with a scan range of 4000 to 400 cm^{-1} and 64 scans.

Fluorescence properties of modified starch films

The fluorescence of the modified starch films was observed using a fully automated inverted fluorescence microscope (Carl Zeiss AG) (Ge et al., 2022).

Analysis of crystallinity of modified starch film

Changes in the crystalline structure of modified starch films were determined using X-ray diffraction (Rigaku). A scan range of $2\theta = 5°–50°$, a step size of 0.05°, and a scan speed of 10°/min were used(Lian, Cao, Jiang, & Rogachev, 2021).

Microstructure analysis of modified starch film

The microscopic morphological characteristics of the samples were assessed by observing the surface and cross-sectional structures of the modified starch films. The surfaces and cross-sections of the modified starch films were sprayed with gold and fixed on a gold spray plate. The surface morphologies and cross-sectional structures of the modified starch film were observed at an accelerating voltage of 5.0 kV.

Analysis of thermal properties of modified starch films

Three to ten milligrams of each modified starch film was tested on a thermogravimetric analyzer (TA, USA). Before analysis, the samples were equilibrated at 25 °C and 53 % RH for 48 h. The films were tested

using high purity nitrogen a flow rate of 50 mL/min, a temperature rise rate of 10 °C/min, and a temperature range of 30–600 °C.

Sweet cherry preservation

OSCS/CS/ZnO/8% ε-PL films were selected for evaluation as a sweet cherry preservative. Cherries with similar ripeness, size, and shape were washed with deionized water to remove surface water. Cherries were set up in the following treatments: without packaging (CK), petroleum film (PE)and OSCS/CS/ZnO/ 8 %ε-PL film (composite film). Five cherries were used per treatment, 3 parallel, and stored at room temperature for 8 days. Cherry appearance was recorded by photographs.

Cherry preservation, decay rate, and stem drying

Fifteen cherries in each treatment were used for decay rate measurements. Data were recorded and decay rate was calculated using regular measurements every-two days as the experiment progressed (Zhang et al., 2021).

$$Decay\ rate(\%) = decayed\ fruits/total\ number\ of\ fruits\ surveyed \times 100\%$$

Fifteen fruits were taken from each treatment, and the fruit pedicel drying levels were assessed every-two days. Fruit pedicel dryness levels were classified into four grades as follows (Zhang et al., 2021).

Grade 0: fruit pedicels were bright green and full of moisture.

Grade 1: fruit pedicels still green but with water loss.

Grade 2: dried area of fruit pedicels less than 2/3.

Grade 3: the dried area of fruit pedicels is more than 2/3, with serious water loss.

Then, fruit pedicel drying index was calculated using the following equation:

$$Fruit\ pedicel\ drying\ index(\%) = \sum(drying\ level \times number\ of\ fruits\ at\ that\ level)/number\ of\ fruits\ inspected \times 100\%$$

Cherry freshness and color

Fifteen cherries in each treatment were fixed for color measurement, and the L*, a*, and b* of the peel were measured on the equatorial part of the cherry surface using a colorimeter (NR110) (Liu, Lin, Lin, Lin, & Fan, 2021), and the data were recorded every-two days as the experiment progressed.

Cherry freshness weight loss rate

Fifteen cherries in each treatment were used to measure the rate of weight loss. Cherries were weighed on an analytical balance, and the weight of each group was measured every-two days as the experiment progressed (Liu et al., 2021). Weight loss rates were calculated according to the following equation:

$$Weight\ loss(\%) = (weight\ of\ cherries\ before\ storage - weight\ of\ cherries\ in\ the\ experiment)/weight\ of\ cherries\ before\ storage \times 100\%$$

Cherry freshness soluble solids

Fifteen cherries in each treatment were used for soluble solids measurement. Soluble solids were measured using a digital display saccharimeter (Qiwei), and the data were recorded every-two days as the experiment progressed (Liu et al., 2021).

Results and discussion

FT-IR spectral analysis of modified starch film

Fig. 1 A shows the FT-IR patterns of the original composites. OSCS, CS, and ε-PL. OSCS is the starch ester obtained by modification of ST by octenyl succinic anhydride, so ST alone was also measured. It is obvious from the IR patterns of OSCS and ST that OSCS produces new peaks of 1725 cm^{-1} and 1572 cm^{-1} that ST does not. The peak at 1725 cm^{-1} is the substitution of –OH by the ester group (Brandelero, Grossmann, & Yamashita, 2012), and the peak at 1572 cm^{-1} is the stretching vibration of RCOO-, which proves that ST was indeed modified to OSCS.

The OSCS/CS film, OSCS/CS/ZnO film, and OSCS/CS/ZnO/ε-PL film all contained characteristic peaks of both OSCS and CS films, with peaks around 2870 cm^{-1} for C—H stretching vibrations and bands around 1074 cm^{-1} for C—O stretching vibrations(Sun et al., 2019).

In the OSCS/CS film, the peak at 1725 cm^{-1} that was present in the CS film disappears, and the peak at 1632 cm^{-1} that was present in the OSCS/CS film is enhanced, probably due to an interaction between the OSCS carbonyl compound and the amino group of CS. The peak at 1632 cm^{-1} in the OSCS/CS/ZnO film is weakened, and ZnO is disrupted for the amide I (Lian et al., 2021). The peaks at 1632 cm^{-1}, 1538 cm^{-1}, and 1258 cm^{-1} in the CS Film are where the amide bond is located (Lian et al., 2021), and the amino peak in CS moves from 1538 cm^{-1} to 1560 cm^{-1}, indicating that there is an interaction between the hydroxyl group of OSCS and the amino group of CS (Lian et al., 2021). The amide bond of ε- PL is located around 1661 cm^{-1}, 1560 cm^{-1}, 1494 cm^{-1}, and 1255 cm^{-1} (L. Zhang et al., 2015). The characteristic peak at 1494 cm^{-1} in ε-PL disappears in the OSCS/CS/ZnO/ε-PL film, and the OSCS/CS/ZnO film is compared to the OSCS/CS/ZnO/ε-PL film and produced a new peak at 1618 cm^{-1}. It is evident that an interaction exists between the amino group of ε-PL and the reducing end of CS, where the Schiff base reaction occurs (Ge et al., 2022; Liang, Yuan, Liu, Wang, & Gao, 2014; Wangprasertkul, Siriwattanapong, & Harnkarnsujarit, 2021).

The broad absorption band located between 3500 cm^{-1} and 3000 cm^{-1} is attributed to the O—H stretching vibration due to inter- and intramolecular hydrogen bonding of hydroxyl groups. The broad band near 3301 cm^{-1} of the OSCS film in Fig. 1B is attributed to the hydroxyl

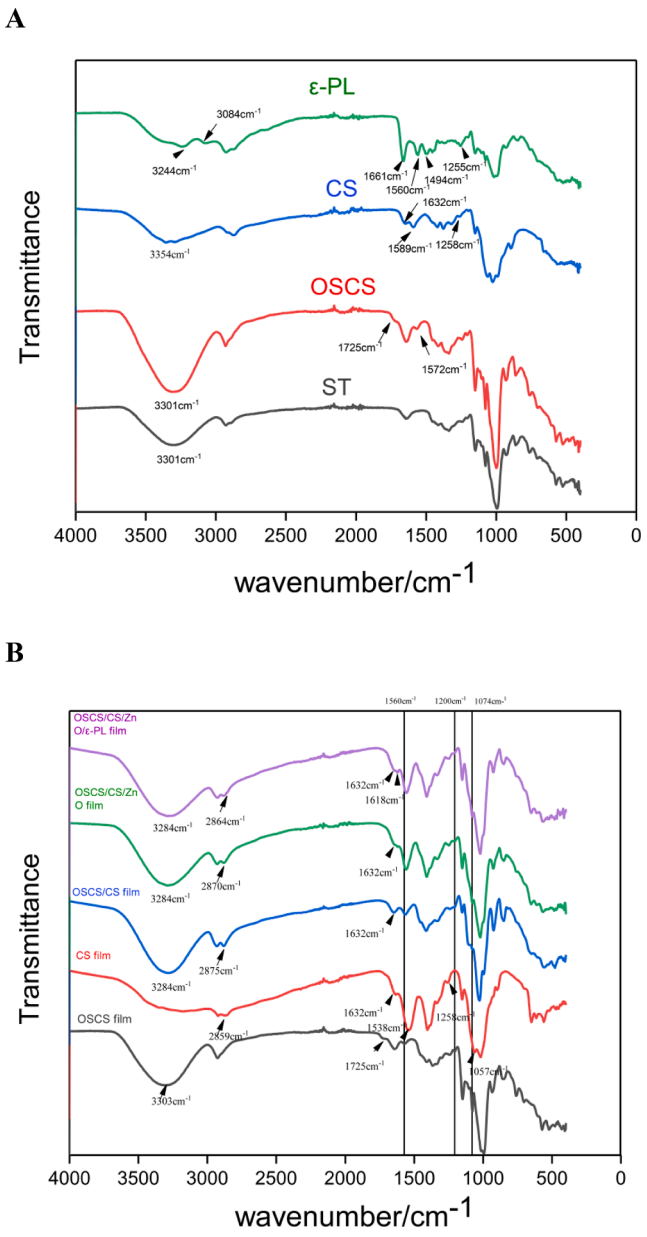

Fig. 1. FT-IR Spectral Analysis of modified starch film.

group in the starch granule, which is red-shifted. Hydrogen bonding is enhanced after the formation of different composite films, from 3301 cm^{-1} in the OSCS film to 3284 cm^{-1} in the OSCS/CS film. This indicates that hydrogen bonds are formed between OSCS and CS. The OSCS/CS/ZnO/ film did not change from the OSCS/CS film, and ZnO was only interspersed between the films as small molecular particles, so the peak

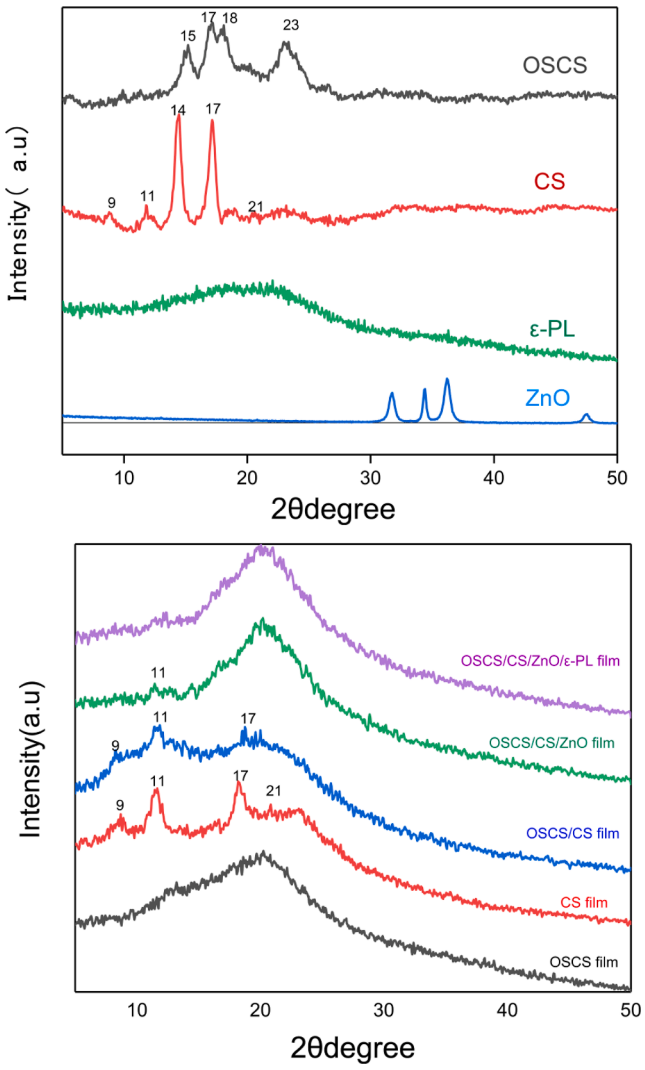

Fig. 3. XRD pattern of modified starch film.

of the band did not change in the OSCS/CS/ZnO film, indicating that hydrogen bonding was not involved in incorporating ZnO (Gao et al., 2022).

Fluorescence properties of modified starch film

The OSCS film had no red fluorescence (Fig. 2A), while both OSCS/CS film (Fig. 2B) and the OSCS/CS/ZnO/ε-PL film (Fig. 2C) had red fluorescence, which is produced by the formation of imine bonds through the Schiff base reaction (Ge et al., 2022). The red fluorescence of the OSCS/CS/ZnO/ε-PL film was stronger, indicating that an interaction occurs between the carbonyl compound of OSCS and the amino

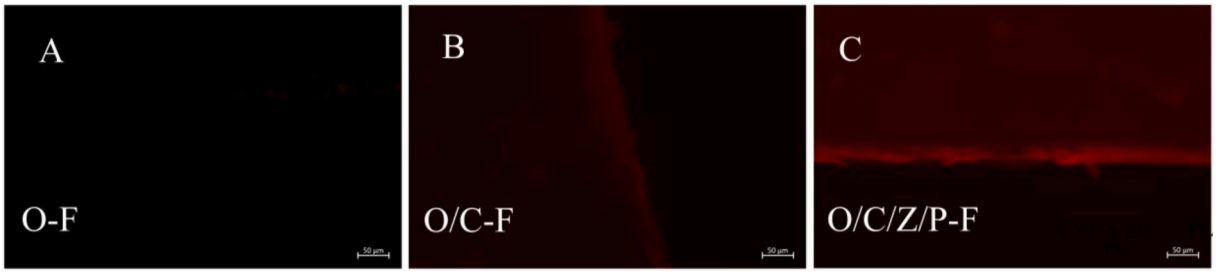

Fig. 2. Fluorescence properties of modified starch film. (A) OSCS Film (O-F); (B) OSCS/CS Film (O/C-F); (C) OSCS/CS/ZnO/ε-PL Film (O/C/Z/P-F).

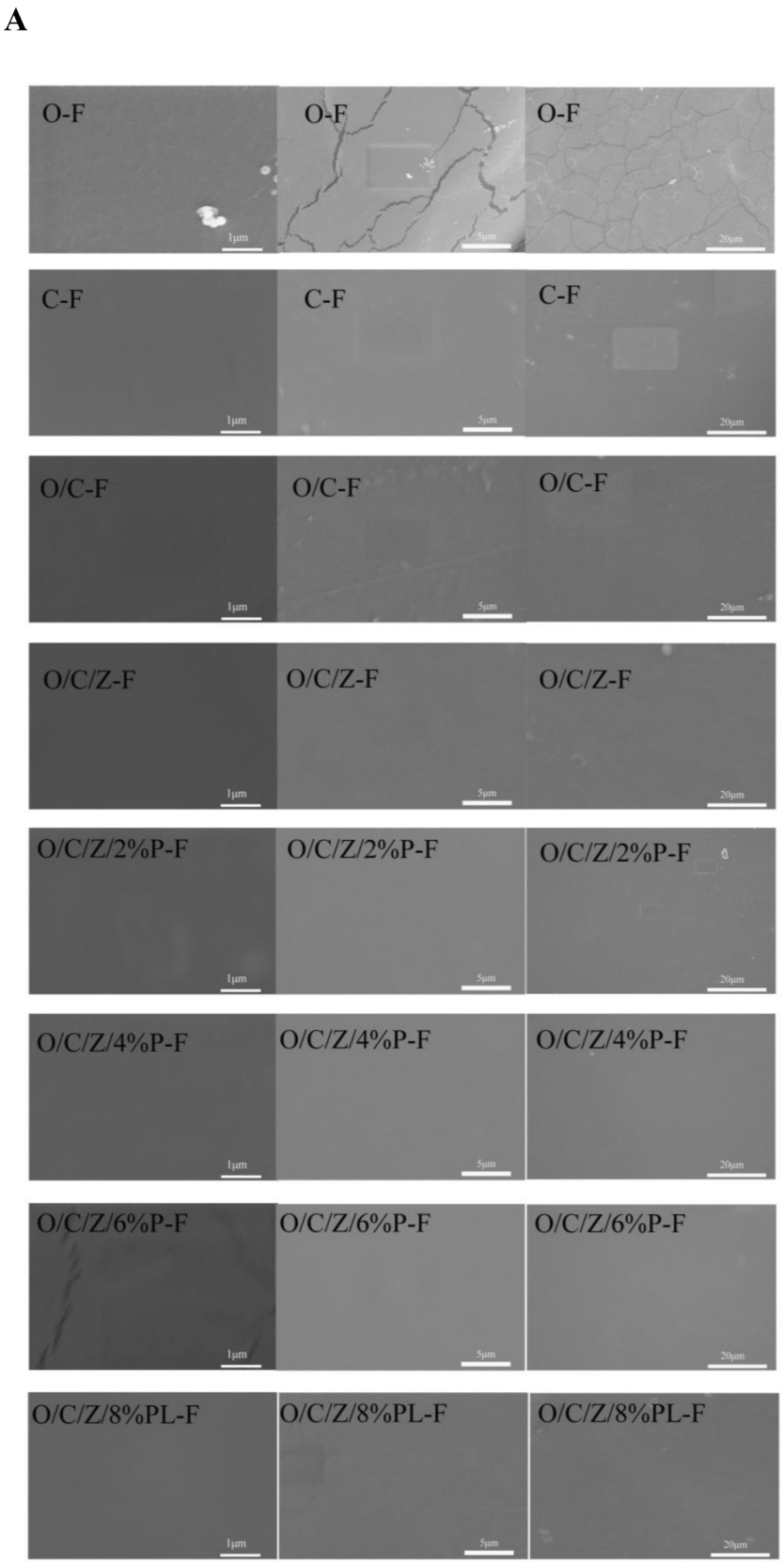

Fig. 4. SEM image of modified starch film. (A) surface view; (B) cross-sectional view. OSCS Film (O-F); CS Film (C-F); OSCS/CS Film(O/C-F); OSCS/CS/ZnO Film (O/C/Z-F); OSCS/CS/ZnO/2% ε-PL Film(O/C/Z/2%P-F); OSCS/CS/ZnO/4% ε-PL Film(O/C/Z/4%P-F); OSCS/CS/ZnO/6% ε-PL Film (O/C/Z/6%P-F); OSCS/CS/ZnO/8% ε-PL Film(O/C/Z/8%P-F).

B

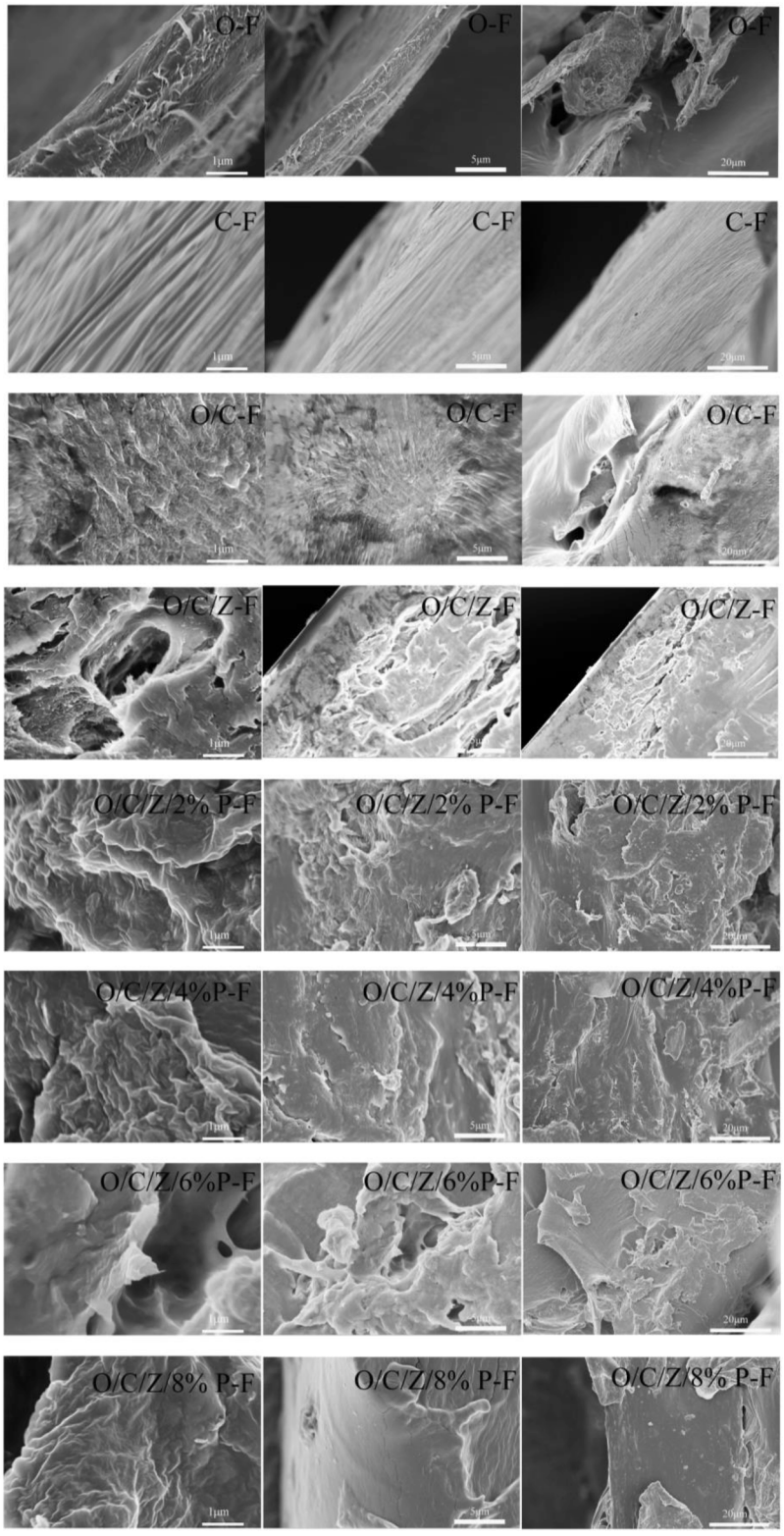

Fig. 4. (*continued*).

group of CS. ε-PL further increases the number of imine bonds. Interactions between the amino group of ε-PL and the reducing end of CS produce a Schiff base reaction (Yuan et al., 2019).

Crystallinity of modified starch film

It can be seen from Fig. 3 that OSCS molecules show diffraction peaks at 2θ = 15°, 17°, 18°, 23.5° for A-type crystals (Lian et al., 2021). For chitosan powder, the two narrow diffraction peaks at 2θ = 9°, 11°, 14°, 17°, 21° are attributed to the semi-crystalline nature of chitosan (Liu, Cai, Jiang, Wu, & Le, 2016). For ε-PL powder, the broad peak at 2θ = 20° indicates a typical amorphous structure (Wu et al., 2019). When the crystalline, semi-crystalline, and amorphous materials in the co-blended films have good miscibility, their crystallinity is lower than that of the individual materials (Omar-Aziz et al., 2021). Crystallinity disappears after paste formation in OSCS films, and some reduction in crystallinity occurs after CS formation. The crystallinity of OSCS/CS and OSCS/CS/ZnO films was further reduced, indicating that OSCS has certain interactions with CS and ZnO. OSCS/CS/ZnO/ε-PL films showed a clear broad diffraction peak with 2θ of 20°, reflecting the fact that the largest part of the film structure is amorphous with a dense network structure between molecules (Gan et al., 2022). This affects the hydrogen bonding of the chitosan itself. The presence of interactions between the amino group of ε-PL and the reducing end of CS causes the film to have lower crystallinity.

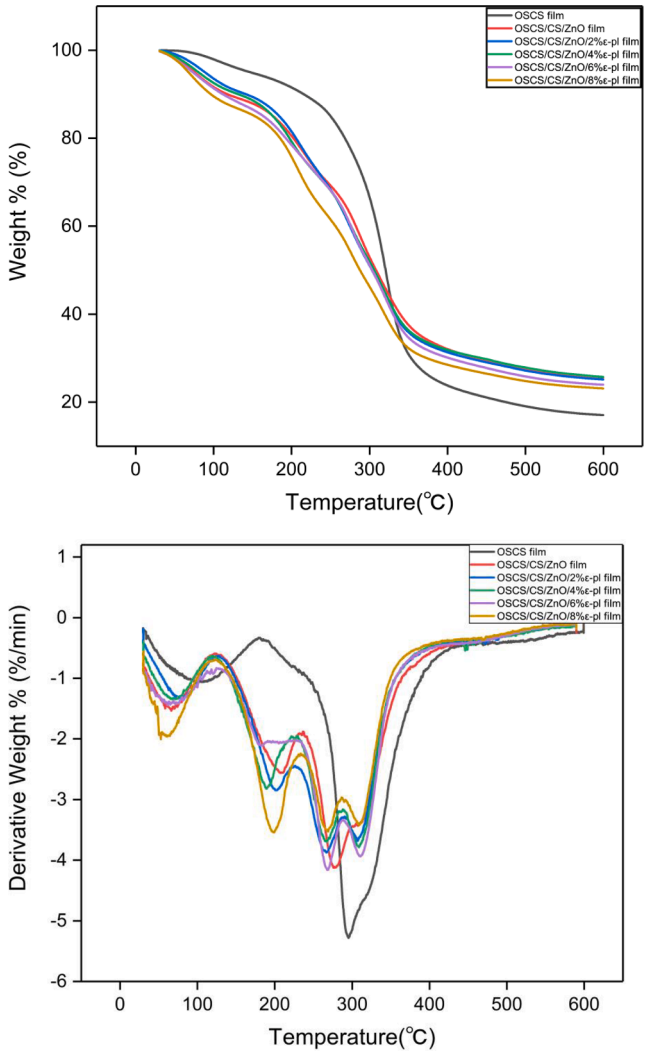

Fig. 5. Thermal stability analysis of modified starch films.

Microstructure of the modified starch film

From Fig. 4, the surfaces of the modified starch films were flat and smooth, and the films had certain apparent structures. The cross-sectional structure of the OSCS film appeared long and ciliated, and the CS film cross-sectional structure was characterized by chain-like aggregation into fibers (Silva-Weiss, Bifani, Ihl, Sobral, & Gómez-Guillén, 2013). The film created by combining OSCS and CS created a groove phenomenon in the cross-sectional structure. The addition of ZnO made the cross-sectional surface of the film more uneven and cavitated, similar to (Hoque, Sarkar, & Ahmed, 2022) findings. The addition of ZnO into the films increases their roughness. With increasing ε-PL content, the cross section of the modified starch films became more polymerized and compact, probably due to interactions between the amino group of ε-PL and the reducing end of CS. Also, ε-PL is a surfactant, enhancing the interaction between the film substrates. The polymer chains were arranged in a more orderly manner by extrusion blowing to prepare ε-poly(lysine hydrochloride) starch/PBAT composite films with new hydrogen bonds formed between ε-PL and starch molecules (Gao et al., 2022), and it was found that the addition of ε-PL resulted in smoother and flatter composite film sections, which ultimately led to better compatibility between substances.

Thermal stability of the modified starch films

Using the thermogravimetric analyzer to study the thermal stability of the film (Fig. 5), we found that the final weight loss of the composite films was lower than that of the pure starch film. The weight loss of the pure starch film reached 82.87 %, and the weight loss of the modified starch composite film was about 72 %, which indicates that the composite film has better thermal stability.

The pure starch film has two decomposition stages. The first stage is the decomposition of water, and the second stage is the breakage of starch molecular chain segments. The OSCS/CS/ZnO film decomposes in three stages. The first stage is the loss of water, the second stage is the loss of substances such as hydroxyl groups after the composite film is bonded, and the third stage is the decomposition of chitosan and starch macromolecular chain segments (Thi Nguyen, Pham, Nhien Le, Bach, & Thuc, 2022). The OSCS/CS/ZnO film with the addition of ε-PL has one more thermal decomposition peak for the decomposition of ε-PL, which is excellent in thermal stability. OSCS/CS/ZnO/ε-PL films with higher ε-PL content showed lower weight loss compared with OSCS/CS/ZnO films and OSCS/CS/ZnO/ε-PL films with lower ε-PL content, indicating that the increase of ε-PL content improved the thermal stability of the composite films. This is because the enhanced intermolecular interactions between ε-PL, CS, and OSCS hinder the accumulation and crystallization of polymer chains, thus lowering the pyrolysis temperature of the polymer (Yu et al., 2019).

Modified starch film freshness preservation effect

We then tested the effect of the different films (CK (no film), PE cling film, and composite film) on cherry preservation. After cherries had been at room temperature for 8 days, Fig. 6A show it was obvious that the CK group had basically all rotted and deteriorated. Cherries in the PE cling film group retained overall brightness and fullness better than cherries in the CK group and composite film group, but they still became moldy. For the modified starch composite film, adding ε-PL inhibitor had excellent anti-mold and freshness effects on cherries.

Cherry preservation decay rate and fruit stem drying index

The degree of fruit decay and pedicel drying index are important indicators of cherry freshness. With longer storage times, the degree of cherry decay and pedicel drying index increased (Fig. 6B). Cherries in the PE group had the highest degree of decay but the lowest pedicel

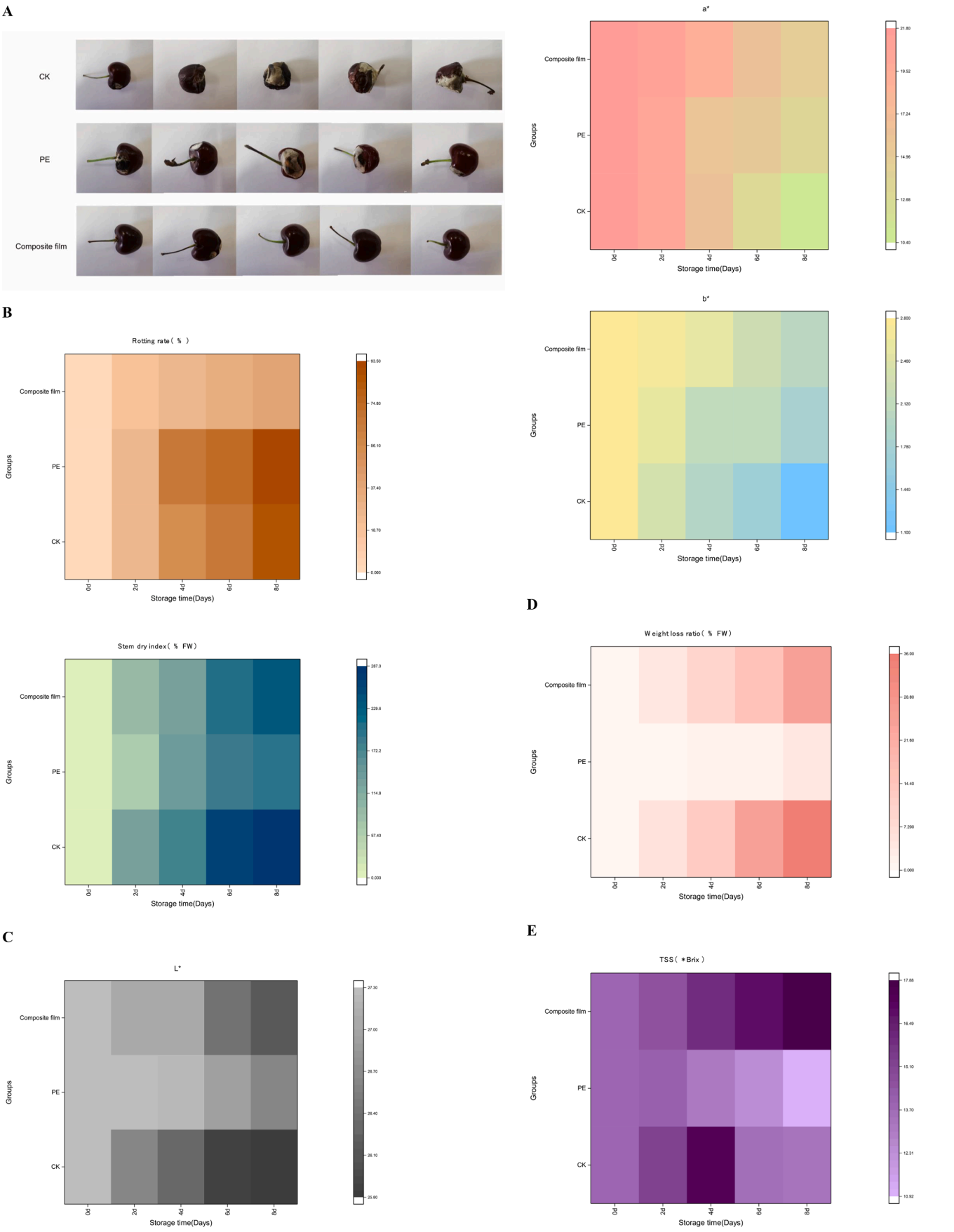

Fig. 6. (A) Freshness preservation effect of modified starch film. (B)Map of cherry preservation decay rate and stem drying index. (C)Cherry preservation color chart. (D)Cherry preservation weight loss rate graph. (E) Soluble solids map for cherry preservation.

drying index because PE cling film has poor permeability. This causes cherries to decay easily but lose very little water. Cherries in the composite film group had the lowest degree of decay, which is related to the inhibition of microorganisms by chitosan, nano-ZnO, and ε-PL. Cherries in the composite film group also had lower stem drying index values than the pure CK group, suggesting that that the bio-based modified starch film slowed down cherry decay and stem drying.

Cherry preservation of color

The main indicators of chromaticity in fruits and vegetables are L*, a* and b*. Brightness and redness are also of great importance for the quality of cherries. From Fig. 6C, it is apparent that throughout the storage and preservation process, cherry peel brightness decreased. As cherries age, the peel turns from bright red to dark red. Cherry peel brightness was higher than the CK group. Overall, a * and b* also showed a decreasing trend in cherry peels treated with the modified starch film. Values of a* and b* were higher in the CK and PE groups than in the modified starch film group due to faster decay in those groups. The a* and b* values of the PE group were higher than those of the CK group, which was related to the low water loss in the non-decayed part of the peel and the bright red color of the fruit. Overall, the modified starch film had the effect of slowing down discoloration.

Cherry weight loss rate during preservation

Weight loss was mainly caused losing water through transpiration. It can be seen from Fig. 6D that with the extension of storage time, the weight loss rate of cherries in all treatment groups gradually increased. The weight loss rate of the CK group increased the fastest, and at 8 d, the weight loss rate of the CK group reached 35.98 %. The weight loss rate of the PE group was the lowest, and at 8 d, the weight loss rate was only 4.17 %. The PE cling film was less permeable, allowing less transpiration to occur. This also led to higher moisture content, which caused decay and deterioration. The modified starch film group reduced water loss and had certain water retention capacity compared to the CK group.

Cherry soluble solids during preservation

"Soluble solids" is a general term for water-soluble compounds, the main component of which is sugar, reflecting the storage quality and maturity of fruits and vegetables. As can be seen from Fig. 6E, with increasing storage time, the soluble solids content of cherries in the CK group showed a trend of first increasing and then decreasing. At 4 d, the content of soluble solids began to decrease. The soluble solids content of the PE group showed a decreasing trend, which might be related to the higher decay and the consumption of sugars by microbes (Chen et al., 2022). The soluble solids content of the composite film group showed an increasing trend, which might be related to the loss of water in cherries, resulting in an increase in the proportion of solids, or it may also be related to the conversion of starch to sugars in the pulp (Schmitz, Freschi, Ferrari, Peroni-Okita, & Cordenunsi-Lysenko, 2022). The soluble solids content of the composite film group was highest during later stages of storage, suggesting that the composite film increases the soluble solids of cherries.

Conclusion

This study used infrared spectroscopy and fluorescence microscopy to demonstrate that the modified starch film was formed by hydrogen bonding and a Schiff base reaction. The narrow diffraction peaks of OSCS at $2\theta = 15^\circ$, 17°, 18°, and 23.5° and peaks of CS at $2\theta = 9^\circ$, 11°, 14°, 17°, 21° disappeared after the formation of thin films. XRD demonstrated that the four materials had good miscibility. Scanning electron microscopy showed that with the increasing ε-PL content, the structure of the modified starch film was more dense, The final weight loss of the composite film was lower than that of the pure starch film, with the weight loss of the pure starch film reaching 82.87 % and the weight loss of the modified starch composite film around 72 %. The structure of the modified starch film had more thermal stability. OSCS/CS/ZnO/8% ε-PL film had the best preservation effect, and the film was successfully applied to cherry preservation. The modified starch film reduced the degree of cherry decay, stem drying, and weight loss rate. By day 8 of cherry storage, the decay rates in the CK and PE groups reached 86.7 % and 93.3 %, respectively, while the decay rate of the modified starch film was only 40 %. For keeping cherry fruit stalks, by day 8, the stem drying index and weight loss in the CK group reached 286.7 % and 36.0 %, respectively, while those in the modified starch film group were only 233.3 % and 24.4 %, respectively. It also maintained the surface color of fruits and vegetables and increased the soluble solids content, bringing it up to 17.8 * Brix. It is a promising alternative to plastic films because it solves many of the problems that plague plastic films, such as difficult degradation and toxicity. It would also reduce production costs and use less resources. The incorporation of ε-PL to in active packaging can provide good protection to food.

Declaration of Competing Interest

The authors declare that they have no known competing financial interests or personal relationships that could have appeared to influence the work reported in this paper.

Data availability

No data was used for the research described in the article.

Acknowledgment

This study was funded by China Agriculture Research System (CARS-11-HNCYH and CARS-11-HNLKM), Hainan Province Science and Technology Special Fund (ZDYF2022XDNY215 and ZDYF2020106) , "National Natural Science Foundation of China (32160529)".

References

Alirezalu, K., Movlan, H. S., Yaghoubi, M., Pateiro, M., & Lorenzo, J. M. (2021). ε-polylysine coating with stinging nettle extract for fresh beef preservation. *Meat Science, 176*, Article 108474. https://doi.org/10.1016/j.meatsci.2021.108474

Blando, F., & Oomah, B. D. (2019). Sweet and sour cherries: Origin, distribution, nutritional composition and health benefits. *Trends in Food Science & Technology, 86*, 517–529. https://doi.org/10.1016/j.tifs.2019.02.052

Brandelero, R. P. H., Grossmann, M. V., & Yamashita, F. (2012). Films of starch and poly (butylene adipate co-terephthalate) added of soybean oil (SO) and Tween 80. *Carbohydrate Polymers, 90*(4), 1452–1460. https://doi.org/10.1016/j.carbpol.2012.07.015

Chang, S.-S., Lu, W.-Y.-W., Park, S.-H., & Kang, D.-H. (2010). Control of foodborne pathogens on ready-to-eat roast beef slurry by ε-polylysine. *International Journal of Food Microbiology, 141*(3), 236–241. https://doi.org/10.1016/j.ijfoodmicro.2010.05.021

Chen, J., Xu, Y., Yi, Y., Hou, W., Wang, L., Ai, Y., … Min, T. (2022). Regulations and mechanisms of 1-methylcyclopropene treatment on browning and quality of fresh-cut lotus (Nelumbo nucifera Gaertn.) root slices. *Postharvest Biology and Technology, 185*, Article 111782. https://doi.org/10.1016/j.postharvbio.2021.111782

Cheng, F., Ai, Y., & Ghosh, S. (2021). Utilization of octenyl succinic anhydride-modified pea and corn starches for stabilizing oil-in-water emulsions. *Food Hydrocolloids, 118*, Article 106773. https://doi.org/10.1016/j.foodhyd.2021.106773

Domínguez-Rodríguez, G., Marina, M. L., & Plaza, M. (2022). In vitro assessment of the bioavailability of bioactive non-extractable polyphenols obtained by pressurized liquid extraction combined with enzymatic-assisted extraction from sweet cherry (Prunus avium L.) pomace. *Food Chemistry, 385*, Article 132688. https://doi.org/10.1016/j.foodchem.2022.132688

El-Naggar, M. E., Hasanin, M., Youssef, A. M., Aldalbahi, A., El-Newehy, M. H., & Abdelhameed, R. M. (2020). Hydroxyethyl cellulose/bacterial cellulose cryogel dopped silver@titanium oxide nanoparticles: Antimicrobial activity and controlled release of Tebuconazole fungicide. *International Journal of Biological Macromolecules, 165*, 1010–1021. https://doi.org/10.1016/j.ijbiomac.2020.09.226

El-Sayed, H. S., El-Sayed, S. M., Mabrouk, A. M. M., Nawwar, G. A., & Youssef, A. M. (2021). Development of eco-friendly probiotic edible coatings based on chitosan, alginate and carboxymethyl cellulose for improving the shelf life of UF soft cheese.

Journal of Polymers and the Environment, 29(6), 1941–1953. https://doi.org/10.1007/s10924-020-02003-3

El-Sayed, H. S., El-Sayed, S. M., & Youssef, A. M. (2021). Novel approach for biosynthesizing of zinc oxide nanoparticles using Lactobacillus gasseri and their influence on microbiological, chemical, sensory properties of integrated yogurt. *Food Chemistry, 365*, Article 130513. https://doi.org/10.1016/j.foodchem.2021.130513

Gan, L., Jiang, G., Yang, Y., Zheng, B., Zhang, S., Li, X., … Peng, B. (2022). Development and characterization of levan/pullulan/chitosan edible films enriched with ε-polylysine for active food packaging. *Food Chemistry, 388*, Article 132989. https://doi.org/10.1016/j.foodchem.2022.132989

Gao, S., Zhai, X., Wang, W., Zhang, R., Hou, H., & Lim, L.-T. (2022). Material properties and antimicrobial activities of starch/PBAT composite films incorporated with ε-polylysine hydrochloride prepared by extrusion blowing. *Food Packaging and Shelf Life, 32*, Article 100831. https://doi.org/10.1016/j.fpsl.2022.100831

Ge, L., Li, Z., Han, M., Wang, Y., Li, X., Mu, C., & Li, D. (2022). Antibacterial dialdehyde sodium alginate/ε-polylysine microspheres for fruit preservation. *Food Chemistry, 387*, Article 132885. https://doi.org/10.1016/j.foodchem.2022.132885

Giménez, M. J., Valverde, J. M., Valero, D., Zapata, P. J., Castillo, S., & Serrano, M. (2016). Postharvest methyl salicylate treatments delay ripening and maintain quality attributes and antioxidant compounds of 'Early Lory' sweet cherry. *Postharvest Biology and Technology, 117*, 102–109. https://doi.org/10.1016/j.postharvbio.2016.02.006

Hoque, M., Sarkar, P., & Ahmed, J. (2022). Preparation and characterization of tamarind kernel powder/ZnO nanoparticle-based food packaging films. *Industrial Crops and Products, 178*, Article 114670. https://doi.org/10.1016/j.indcrop.2022.114670

Jayakumar, A., Radoor, S., Kim, J. T., Rhim, J. W., Nandi, D., Parameswaranpillai, J., & Siengchin, S. (2022). Recent innovations in bionanocomposites-based food packaging films – A comprehensive review. *Food Packaging and Shelf Life, 33*, Article 100877. https://doi.org/10.1016/j.fpsl.2022.100877

Jiao, W., Liu, X., Chen, Q., Du, Y., Li, Y., Yue, F., … Fu, M. (2020). Epsilon-poly-l-lysine (ε-PL) exhibits antifungal activity in vivo and in vitro against Botrytis cinerea and mechanism involved. *Postharvest Biology and Technology, 168*, Article 111270. https://doi.org/10.1016/j.postharvbio.2020.111270

Lian, R., Cao, J., Jiang, X., & Rogachev, A. V. (2021). Physicochemical, antibacterial properties and cytocompatibility of starch/chitosan films incorporated with zinc oxide nanoparticles. *Materials Today Communications, 27*, Article 102265. https://doi.org/10.1016/j.mtcomm.2021.102265

Liang, C., Yuan, F., Liu, F., Wang, Y., & Gao, Y. (2014). Structure and antimicrobial mechanism of ε-polylysine–chitosan conjugates through Maillard reaction. *International Journal of Biological Macromolecules, 70*, 427–434. https://doi.org/10.1016/j.ijbiomac.2014.07.012

Liu, J., Lin, Y., Lin, H., Lin, M., & Fan, Z. (2021). Impacts of exogenous ROS scavenger ascorbic acid on the storability and quality attributes of fresh longan fruit. *Food Chemistry: X, 12*, Article 100167. https://doi.org/10.1016/j.fochx.2021.100167

Liu, Q., Li, Y., Xing, S., Wang, L., Yang, X., Hao, F., & Liu, M. (2022). Genipin-crosslinked amphiphilic chitosan films for the preservation of strawberry. *International Journal of Biological Macromolecules, 213*, 804–813. https://doi.org/10.1016/j.ijbiomac.2022.06.037

Liu, Y., Cai, Y., Jiang, X., Wu, J., & Le, X. (2016). Molecular interactions, characterization and antimicrobial activity of curcumin–chitosan blend films. *Food Hydrocolloids, 52*, 564–572. https://doi.org/10.1016/j.foodhyd.2015.08.005

Moustafa, H., Darwish, N. A., & Youssef, A. M. (2022). Rational formulations of sustainable polyurethane/chitin/rosin composites reinforced with ZnO-doped-SiO2 nanoparticles for green packaging applications. *Food Chemistry, 371*, Article 131193. https://doi.org/10.1016/j.foodchem.2021.131193

Omar-Aziz, M., Gharaghani, M., Hosseini, S. S., Khodaiyan, F., Mousavi, M., Askari, G., & Kennedy, J. F. (2021). Effect of octenylsuccination of pullulan on mechanical and barrier properties of pullulan-chickpea protein isolate composite film. *Food Hydrocolloids, 121*, Article 107047. https://doi.org/10.1016/j.foodhyd.2021.107047

Pan, L., Chen, X., Xu, W., Fan, S., Wan, T., Zhang, J., & Cai, Y. (2022). Methyl jasmonate induces postharvest disease resistance to decay caused by Alternaria alternata in sweet cherry fruit. *Scientia Horticulturae, 292*, Article 110624. https://doi.org/10.1016/j.scienta.2021.110624

Rahman, S., Konwar, A., Majumdar, G., & Chowdhury, D. (2021). Guar gum-chitosan composite film as excellent material for packaging application. *Carbohydrate Polymer Technologies and Applications, 2*, Article 100158. https://doi.org/10.1016/j.carpta.2021.100158

Schmitz, G. J. H., Freschi, L., Ferrari, R. C., Peroni-Okita, F. H. G., & Cordenunsi-Lysenko, B. R. (2022). Exploring the significance of photosynthetic activity and carbohydrate metabolism in peel tissues during banana fruit ripening. *Scientia Horticulturae, 295*, Article 110811. https://doi.org/10.1016/j.scienta.2021.110811

Sharma, P., Gaur, V. K., Gupta, S., Varjani, S., Pandey, A., Gnansounou, E., … Wong, J. W. C. (2022). Trends in mitigation of industrial waste: Global health hazards, environmental implications and waste derived economy for environmental sustainability. *Science of The Total Environment, 811*, Article 152357. https://doi.org/10.1016/j.scitotenv.2021.152357

Silva-Weiss, A., Bifani, V., Ihl, M., Sobral, P. J. A., & Gómez-Guillén, M. C. (2013). Structural properties of films and rheology of film-forming solutions based on chitosan and chitosan-starch blend enriched with murta leaf extract. *Food Hydrocolloids, 31*(2), 458–466. https://doi.org/10.1016/j.foodhyd.2012.11.028

Sun, H., Shao, X., Zhang, M., Wang, Z., Dong, J., & Yu, D. (2019). Mechanical, barrier and antimicrobial properties of corn distarch phosphate/nanocrystalline cellulose films incorporated with Nisin and ε-polylysine. *International Journal of Biological Macromolecules, 136*, 839–846. https://doi.org/10.1016/j.ijbiomac.2019.06.134

Thi Nguyen, T., Pham, B.-T.-T., Nhien Le, H., Bach, L. G., & Thuc, C. N. H. (2022). Comparative characterization and release study of edible films of chitosan and natural extracts. *Food Packaging and Shelf Life, 32*, Article 100830. https://doi.org/10.1016/j.fpsl.2022.100830

Wang, D., Sun, J., Li, J., Sun, Z., Liu, F., Du, L., & Wang, D. (2022). Preparation and characterization of gelatin/zein nanofiber films loaded with perillaldehyde, thymol, or ε-polylysine and evaluation of their effects on the preservation of chilled chicken breast. *Food Chemistry, 373*, Article 131439. https://doi.org/10.1016/j.foodchem.2021.131439

Wang, X., Huang, X., Zhang, F., Hou, F., Yi, F., Sun, X., … Liu, Z. (2022). Characterization of chitosan/zein composite film combined with tea polyphenol and its application on postharvest quality improvement of mushroom (Lyophyllum decastes Sing.). *Food Packaging and Shelf Life, 33*, Article 100869. https://doi.org/10.1016/j.fpsl.2022.100869

Wangprasertkul, J., Siriwattanapong, R., & Harnkarnsujarit, N. (2021). Antifungal packaging of sorbate and benzoate incorporated biodegradable films for fresh noodles. *Food Control, 123*, Article 107763. https://doi.org/10.1016/j.foodcont.2020.107763

Wu, C., Sun, J., Lu, Y., Wu, T., Pang, J., & Hu, Y. (2019). In situ self-assembly chitosan/ε-polylysine bionanocomposite film with enhanced antimicrobial properties for food packaging. *International Journal of Biological Macromolecules, 132*, 385–392. https://doi.org/10.1016/j.ijbiomac.2019.03.133

Wu, D., Li, Q., Shang, X., Liang, Y., Ding, X., Sun, H., … Chen, J. (2021). Commodity plastic burning as a source of inhaled toxic aerosols. *Journal of Hazardous Materials, 416*, Article 125820. https://doi.org/10.1016/j.jhazmat.2021.125820

Xie, Y., Pan, Y., & Cai, P. (2022). Cellulose-based antimicrobial films incroporated with ZnO nanopillars on surface as biodegradable and antimicrobial packaging. *Food Chemistry, 368*, Article 130784. https://doi.org/10.1016/j.foodchem.2021.130784

You, M., Duan, X., Li, X., Luo, L., Zhao, Y., Pan, H., … Li, G. (2022). Effect of 1-Methylcyclopropene combined with chitosan-coated film on storage quality of passion fruit. *Sustainable Chemistry and Pharmacy, 27*, Article 100679. https://doi.org/10.1016/j.scp.2022.100679

Youssef, A. M., Abdel-Aziz, M. S., & El-Sayed, S. M. (2014). Chitosan nanocomposite films based on Ag-NP and Au-NP biosynthesis by Bacillus Subtilis as packaging materials. *International Journal of Biological Macromolecules, 69*, 185–191. https://doi.org/10.1016/j.ijbiomac.2014.05.047

Youssef, A. M., El-Sayed, H. S., El-Nagar, I., & El-Sayed, S. M. (2021). Preparation and characterization of novel bionanocomposites based on garlic extract for preserving fresh Nile tilapia fish fillets. *RSC ADVANCES, 11*(37), 22571–22584. https://doi.org/10.1039/d1ra03819b

Youssef, A. M., & El-Sayed, S. M. (2018). Bionanocomposites materials for food packaging applications: Concepts and future outlook. *Carbohydrate Polymers, 193*, 19–27. https://doi.org/10.1016/j.carbpol.2018.03.088

Yu, Z., Rao, G., Wei, Y., Yu, J., Wu, S., & Fang, Y. (2019). Preparation, characterization, and antibacterial properties of biofilms comprising chitosan and ε-polylysine. *International Journal of Biological Macromolecules, 141*, 545–552. https://doi.org/10.1016/j.ijbiomac.2019.09.035

Yuan, L., Li, X., Ge, L., Jia, X., Lei, J., Mu, C., & Li, D. (2019). Emulsion template method for the fabrication of gelatin-based scaffold with a controllable pore structure. *ACS Applied Materials & Interfaces, 11*(1), 269–277. https://doi.org/10.1021/acsami.8b17555

Zhang, L., Li, R., Dong, F., Tian, A., Li, Z., & Dai, Y. (2015). Physical, mechanical and antimicrobial properties of starch films incorporated with ε-poly-l-lysine. *Food Chemistry, 166*, 107–114. https://doi.org/10.1016/j.foodchem.2014.06.008

Zhang, Y.-L., Cui, Q.-L., Wang, Y., Shi, F., Liu, Y.-P., Liu, J.-L., & Nie, G.-W. (2021). Effect of carboxymethyl chitosan-gelatin-based edible coatings on the quality and antioxidant properties of sweet cherry during postharvest storage. *Scientia Horticulturae, 289*, Article 110462. https://doi.org/10.1016/j.scienta.2021.110462